Age-Associated Resilience Against Ischemic Injury in Mice Exposed to Transient Middle Cerebral Artery Occlusion

Mustafa C. Beker[1,2] · Fatmagul I. Aydinli[1,2,3] · Ahmet B. Caglayan[2,4] · Merve Beker[5] · Oguzhan Baygul[1,2] · Aysun Caglayan[1,2] · Aurel Popa-Wagner[6] · Thorsten R. Doeppner[7] · Dirk M. Hermann[8] · Ertugrul Kilic[1,2,9]

Abstract

Ischemic stroke is the leading cause of death and disability. Although stroke mainly affects aged individuals, animal research is mostly one on young rodents. Here, we examined the development of ischemic injury in young (9–12-week-old) and adult (72-week-old) C57BL/6 and BALB/c mice exposed to 30 min of intraluminal middle cerebral artery occlusion (MCAo). Post-ischemic reperfusion did not differ between young and adult mice. Ischemic injury assessed by infarct area and blood-brain barrier (BBB) integrity assessed by IgG extravasation analysis was smaller in adult compared with young mice. Microvascular viability and neuronal survival assessed by CD31 and NeuN immunohistochemistry were higher in adult than young mice. Tissue protection was associated with stronger activation of cell survival pathways in adult than young mice. Microglial/macrophage accumulation and activation assessed by F4/80 immunohistochemistry were more restricted in adult than young mice, and pro- and anti-inflammatory cytokine and chemokine responses were reduced by aging. By means of liquid chromatography-mass spectrometry, we identified a hitherto unknown proteome profile comprising the upregulation of glycogen degradation-related pathways and the downregulation of mitochondrial dysfunction-related pathways, which distinguished post-ischemic responses of the aged compared with the young brain. Our study suggests that aging increases the brain's resilience against ischemic injury.

✉ Ertugrul Kilic
ertugrul.kilic@medeniyet.edu.tr

1 Department of Physiology, School of Medicine, Istanbul Medipol University, Istanbul, Turkey

2 Research Institute for Health Sciences and Technologies (SABITA), Istanbul Medipol University, Istanbul, Turkey

3 Department of Medical Biology, School of Medicine, Nisantasi University, Istanbul, Turkey

4 Department of Physiology, International School of Medicine, Istanbul Medipol University, Istanbul, Turkey

5 Department of Medical Biology, International School of Medicine, University of Health Sciences, Istanbul, Turkey

6 Experimental Research Center for Normal and Pathological Aging, ARES, University of Medicine and Pharmacy Craiova, Craiova, Romania

7 Department of Neurology, University of Giessen, Giessen, Germany

8 Department of Neurology, University Hospital Essen, University of Duisburg-Essen, Essen, Germany

9 Department of Physiology, Faculty of Medicine, Istanbul Medeniyet University, Unalan, TR-34700 Istanbul, Turkey

Abbreviations

MCAo	Middle cerebral artery occlusion
CNS	Central nervous system
BBB	Blood-brain barrier
CBF	Cerebral blood flow
LDF	Laser Doppler flowmetry
PBS	Phosphate-buffered saline
PFA	Paraformaldehyde
BSA	Bovine serum albumin
PECAM/CD31	Platelet endothelial cell adhesion molecule
FASP	Filter-aided sample preparation
LC-MS/MS	Liquid chromatography-mass spectrometry
FA	Formic acid
ACN	Acetonitrile
IMS	Ion mobility separation
IPA	Ingenuity pathway analysis
TBS	Tris-buffered saline
SD	Standard deviation
ROS	Reactive oxygen species

ROI	Regions of interest
G-CSF	Granulocyte colony-stimulating factor
GM-CSF	Granulocyte macrophage-colony stimulating factor
IL-1β	Interleukin 1 beta
IL-1ra	Interleukin 1 receptor antagonist
IL-2	Interleukin 2
IL-3	Interleukin 3
IL-4	Interleukin 4
IL-5	Interleukin 5
IL-6	Interleukin 6
IL-7	Interleukin 7
IL-10	Interleukin 10
IL-12p70	Interleukin-12 p70
IL-13	Interleukin 13
IL-16	Interleukin 16
IL-17	Interleukin 17
IL-23	Interleukin 23
IL-27	Interleukin 27
TNF-α	Tumor necrosis factor alpha
TREM-1	Triggering receptor expressed on myeloid cells 1
IFN-γ	Interferon gamma
I-309	Chemokine (C-C motif) ligand 1
BLC	B lymphocyte chemoattractant
CXCL10	C-X-C motif chemokine ligand 10
CXCL11	C-X-C motif chemokine 11
CXCL1	C-X-C motif chemokine ligand 1
MIG	Monokine induced by gamma-interferon
MIP-1α	Macrophage inflammatory protein-1 alpha
MIP-1β	Macrophage inflammatory protein-1 beta
MIP-2	Macrophage inflammatory protein 2
RANTES	Regulated upon activation normal T cell expressed and presumably secreted
MCP-1	Monocyte chemoattractant protein-1
MCP-5	Monocyte chemoattractant protein-5
SDF-1	Stromal cell-derived factor 1
PTEN	Phosphatase and tensin homolog
GSK3	Glycogen synthase kinase-3
PARK7	Parkinsonism associated deglycase
HSPA8	Heat shock protein family member 8

Introduction

Ischemic stroke is the leading cause of long-term disability and a prevalent cause of death worldwide [1]. Each year, approximately 15 million people worldwide suffer an ischemic stroke [2], and the number of humans affected is still rising due to increasing life expectancy [3]. Clinical studies suggest that the mechanisms of ischemic injury may differ between young and aged patients [4]. For studying mechanisms underlying

ischemic brain injury, rodent models are widely used [5]. Intraluminal middle cerebral artery occlusion (MCAo) is a widely used model that allows for inducing reproducible ischemias followed by standardized reperfusions [6]. Due to surgical challenges, intraluminal MCAo is mostly performed on young animals [7, 8]. These studies poorly mimic the situation of aged patients. Insufficient knowledge regarding the situation in the aged brain is currently regarded as a major reason that hampers therapeutic progress in the ischemic stroke field [9].

Only a few studies so far examined age-related mechanisms of injury in the ischemic brain [10–13]. Existing studies provide a heterogeneous picture of injury responses. Some studies showed that ischemic brain injury was more severe in young than old animals [10, 13, 14], while other studies found no age-related differences [15, 16] and again other studies, including an own study, observed that ischemic injury was more severe in old than young animals [9, 12, 17, 18]. In our own study, post-ischemic reperfusion, assessed by laser Doppler flowmetry (LDF), was reduced in adult compared with young mice [9]. The impaired reperfusion most likely explains the more severe brain injury. In previous stroke studies, the C57BL/6 mouse was the most common mouse strain. Strain differences may be determinants of injury responses post-ischemia.

Focal cerebral ischemia initiates an inflammatory cascade in which cytokines and chemokines are essential mediators [19]. In the central nervous system (CNS), resident microglia, the principal brain-derived immune cells, are the first cells to respond to the pathophysiological alterations induced by ischemia [20]. Both microglial activation and blood-brain barrier (BBB) degradation enable the brain infiltration of blood-derived leukocytes including neutrophils, monocytes, and macrophages [21], which aggravate ischemic brain injury [22]. Injury development after ischemic stroke is directly related to cell signaling responses [23]. Meanwhile, proteomics is widely used for studying protein responses to ischemia [23, 24]. Cell signaling responses have so far not been analyzed systematically in the aged compared with the young ischemic brain.

In this study, we used young (that is, 9–12-week-old) and adult (that is, 72-week-old) C57BL/6 and BALB/c mice for evaluating the effect of age on ischemic brain injury induced by 30 min intraluminal MCAo. Ischemic brain injury, BBB integrity, and immunological responses were assessed by immunohistochemistry. Cytokine and chemokine responses were examined by a broad cytokine array, and cell signaling was analyzed by proteome analysis and Western blotting.

Materials and Methods

Ethics Statement

This study has been conducted under the ethics standards of the EU Guidelines on the Care and Use of Laboratory

Animals (Directive 2010/63/EU) in agreement with local guidelines and legislation. The study has been approved by the Animal Research Ethics Committee of Istanbul Medipol University (approval number: 08062017-33). Experiments were performed using young (9–12-week-old) and adult (72-week-old) male C57BL/6 and BALB/c mice. All animals were maintained under a constant 12:12-h light-darkness regimen with ad libitum access to food and water. All mice were randomly assigned to experimental groups.

Animal Surgery

Mice were anesthetized with 1% isoflurane (30% O_2, reminder N_2O), and rectal temperature was stabilized between 36.5 and 37°C using a feedback-controlled heating system. During the experiments, cerebral blood flow (CBF) was monitored via laser Doppler flowmetry (LDF) using a flexible 0.5-mm fiber optic probe (Perimed, Sweden) attached with tissue adhesive to the intact skull overlying the core of the middle cerebral artery (MCA) territory (2 mm posterior and 6 mm lateral from bregma). Focal cerebral ischemia was induced using an intraluminal filament technique [25]. Briefly, after a midline neck incision, the left common and external carotid arteries were isolated and ligated. A microvascular clip (FE691, Aesculap, Center Valley, PA, USA) was temporarily placed on the internal carotid artery. A 7-0 silicon-coated nylon monofilament (701934PK5Re, Doccol, MA, USA) was inserted through a small incision into the common carotid artery and advanced 9 mm distal to the carotid bifurcation for MCAo. Thirty minutes later, reperfusion was initiated by monofilament removal. Mice were placed back into their home cages and sacrificed 72 h after the onset of ischemia.

Serum IgG Extravasation Measurement

Brain sections from the bregma level of young and adult mice were gently rinsed for 10 min at room temperature in 0.1 M phosphate-buffered saline (PBS) to remove intravascular IgG and were fixed in 4% paraformaldehyde (PFA) [26]. Following the blocking of endogenous peroxidase with methanol/0.3% H_2O_2 and immersion in 0.1 M PBS containing 5% bovine serum albumin (BSA) and normal swine serum (1:1000), sections were incubated for 1 h in biotinylated goat anti-mouse IgG (sc-2013; Santa Cruz Biotechnology, Dallas, TX, USA) and stained with an avidin peroxidase kit (PK-6100, Vectastain Elite, Newark, CA, USA) and diaminobenzidine (D6815, Sigma Aldrich, St. Louis, MO, USA). For reasons of data comparability, all sections were processed in parallel. Sections were scanned, and the area of IgG extravasation in the ischemic hemisphere was analyzed [27].

Determination of Neuronal Survival, Capillary Density, and Microglial/Macrophage Responses

Brain sections of young and adult mice were fixed in 4% PFA /0.1 M PBS, washed, and immersed for 1 h in 0.1 M PBS containing 0.3% Triton X and 10% normal goat serum. Sections were incubated overnight at 4°C with Alexa Fluor 488-conjugated monoclonal mouse anti-NeuN (Mab377X; Millipore, Burlington, MA, USA, 1:100), FITC conjugated monoclonal rat cluster of disease/anti-platelet endothelial cell adhesion molecule (CD31/PECAM-1; sc-376764, Santa Cruz Biotechnology, 1:200), and Alexa Fluor 488-conjugated monoclonal anti-F4/80 (53-481-82, Thermo Scientific, Waltham, MA, USA, 1:500) antibody. The next day, sections were counterstained with 4',6-diamidino-2-phenylindole (DAPI; D9542, Sigma Aldrich). Images were acquired on a confocal Zeiss LSM 780 microscope (Carl Zeiss, Jena, Germany). Nine different regions of interest (ROIs) in the striatum, each measuring 62,500 μm^2, were evaluated. Mean numbers of $NeuN^+$ cells were determined in the ischemic and contralesional striatum. From results obtained in both hemispheres, the percentage of surviving neurons in the ischemic striatum was determined [28]. $F4/80^+$ microglial cells/macrophages were determined in the same ROIs. For quantification of $CD31^+$ microvessels profile, ten different ROIs in the contralesional striatum, each measuring 400.00 μm^2, were evaluated. We have assigned it as square. A total of 400 μm^2 area per point was drawn by a grid. $CD31^+$ signals on the vertical line were counted.

Analysis of Infarct Area and Brain Swelling

To determine the infarct area and brain swelling, coronal brain sections obtained from striatum were stained with Cresyl violet [26]. The border between infarcted and non-infarcted tissue was outlined using an image analysis system (Image J; National Institute of Health, Bethesda, USA). Infarct areas were assessed by subtracting the areas of the non-infarcted ipsilesional hemisphere from those of the contralesional side. By integrating infarct areas across various rostrocaudal levels, total infarct area was calculated. Brain swelling was determined by calculating total area differences between the ischemic and nonischemic hemispheres.

Cytokine Array

Tissue samples of the ischemic striatum of C57BL/6 mice were harvested, homogenized, sonicated, and then treated with a protease/phosphatase inhibitor cocktail (5872, Cell Signaling Technologies, Danvers, MA, USA) for protein protection. Cytokine levels were analyzed by the Proteome Profiler Mouse Cytokine Array Panel A kit (R&D Systems, Minneapolis, MN, USA). Protein levels for CXCL13/

BLC/BCA-1, C5a, G-CSF, GM-CSF, CCL1/I-309, CCL11/eotaxin, ICAM-1, IFN-γ, IL-1α /IL-1F1, IL-1β /IL-1F2, IL-1ra/IL-1F3, IL-2, IL-3, IL-4, IL-5, IL-6, IL-7, IL-10, IL-12 p70, IL-13, IL-16, IL-17, IL-23, IL-27, CXCL10/IP-10, CXCL11/I-TAC, CXCL1/KC, M-CSF, CCL2/JE/MCP-1, CCL12/MCP-5, CXCL9/MIG, CCL3/MIP-1α, CCL4/MIP-1β, CXCL2/MIP-2, CCL5/RANTES, CXCL12/SDF-1, CCL17/TARC, TIMP-1, TNF-α, and TREM-1 were densitometrically analyzed using the ChemiDoc MP System (1708280, Bio-Rad, Hercules, CA, USA) by Image J software. Data were calibrated with values determined on positive controls.

Sample Preparation for Liquid Chromatography-Mass Spectrometry

Sample preparation was performed as previously described [28] using brain tissue samples obtained from the ischemic striatum of C57BL/6 mice. Tryptic peptides were generated according to the Filter Aided Sample Preparation Protocol (FASP) [29]. Brain tissue from the ischemic striatum was homogenized in 50 mM ammonium bicarbonate and lysed by heating at 95°C in UPX buffer (Expedeon, Germany). After incubation at 4°C for 1 h, samples were centrifuged at 14,000g for 10 min, and the supernatants were transferred to clean 1.5 ml microcentrifuge tubes. The total protein concentration was measured with a Qubit assay. Tryptic peptides were generated by the FASP kit (Expedeon, Germany). Briefly, 50 μg protein was filtered with 6 M urea in a 30 kDa cut-off spin column, alkylated with 10 mM iodoacetamide in the dark for 20 min at room temperature, incubated with trypsin (1:100 trypsin to protein ratio, 90057, Thermo Scientific) overnight at 37°C. The tryptic peptides were eluted from the columns and lyophilized. The peptides were re-dissolved in 0.1% formic acid (FA, Sigma Aldrich) and diluted to 100 ng/μl before injecting into the LC-MS/MS system [25].

LC-MS/MS Analysis and Data Processing

Subsequent protein identifications with LC-MS/MS were performed according to a previously published protocol [25, 30, 31]. The tryptic peptides were loaded onto the ACQUITY UPLC M-Class coupled to an SYNAPT G2-Si high-definition mass spectrometer (Waters, Milford, MA, USA). The columns were equilibrated with 97% mobile phase A (0.1% FA in UHPLC grade water, Merck, Whitehouse, NJ, USA), and the temperature was set to 55°C. Peptides were separated by a 90 min gradient elution from the trap column (Symmetry C18, 5 μm, 180 μm i.d. × 20 mm, Waters) to the analytic column (CSH C18, 1.7 μm, 75 μm i.d. × 250 mm, Waters) at 0.400 μl/min flow rate with a gradient from 4 to 40% acetonitrile (ACN) containing 0.1% FA (v/v). Positive ion modes of MS and MS/MS scans with 0.7 s cycle time were performed sequentially. Ten volts was set as low collision energy, while 30 V was set as high collision energy (CE). The ions were separated by ion mobility separation (IMS). Wave velocity was ramped from 1000 to 55 m/s over the full IMS cycle. The release time for mobility trapping was set as 500 μs, and the trap height was set to 15 V. IMS wave delay was 1000 μs for the mobility separation after trap release [32]. Without any precursor ion preselection, all the ions within the 50–1900 m/z range were fragmented in resolution mode. Additionally, 100 fmol/μl Glu-1-fibrinopeptide B was infused as lock mass reference with a 60 s interval. Progenesis-QI for proteomics software (Waters) was used to identify and quantify the peptides. At least two unique peptide sequences identified all proteins, then the *p*-values and expression ratio of proteins were calculated [25, 28]. Heat maps were generated by GraphPad Prism 9. For protein classification and molecular function analysis, Panther software was used. Protein-protein interaction was done by STRING software. The confidence score was set at 0.4. The Ingenuity Pathway Analysis (IPA) system (version 42012434, Ingenuity Systems; Qiagen China Co., Ltd.) was used for canonical pathway analysis. The −log (*p*-value) >1.3 was taken as the threshold for canonical pathway analysis, and disease and function analysis.

Western Blot

As previously described [25, 26], harvested tissue samples from the ischemic striatum of C57BL/6 mice were pooled, homogenized, sonicated, and then treated with a protease/phosphatase inhibitor cocktail (5872, Cell Signaling Technologies). Total protein content was evaluated using Qubit 3.0 Fluorometer (Q33216, Invitrogen, Waltham, MA, USA). Equal amounts of protein (20 μg) were size-fractionated using 4–20% Mini-PROTEAN TGX (4561096, Bio-Rad) gel electrophoresis and then transferred to a PVDF membrane using the Trans-Blot Turbo Transfer System (1704155, Bio-Rad). After that, membranes were blocked in 5% non-fat milk in 50 mM Tris-buffered saline (TBS) containing 0.1% Tween (TBS-T; blocking solution) for 1 h at room temperature and washed in 50 mM TBS-T. Membranes were incubated overnight with the following primary antibodies: polyclonal rabbit anti-phosphorylated Akt (9275, Cell Signaling Technologies, 1:1000), monoclonal rabbit anti-phosphorylated p44/42 mitogen-activated protein kinase (MAPK)/extracellular-regulated kinase-1/2 (ERK1/2) (4370; Cell Signaling Technologies), polyclonal

rabbit anti-phosphorylated phosphatase and tensin homolog (p-PTEN) (9551, Cell Signaling Technologies), monoclonal rabbit anti-phosphorylated glycogen synthase kinase-3β (p-GSK3β) (5558, Cell Signaling Technologies), and polyclonal rabbit anti-Bcl-xL (2762, Cell Signaling Technologies). The next day, membranes were washed with 50 mM TBS-T and incubated with horseradish peroxidase-conjugated goat-anti-rabbit (sc-2004, Santa Cruz Biotechnology) antibody (diluted 1:2500) for 1 h at room temperature. Blots were performed at least three times. Protein loading was controlled by stripping and re-probing the membranes with polyclonal rabbit anti-β-actin antibody (4967, Cell Signaling Technologies). Blots were developed using the Clarity Western ECL Substrate kit (1705060, Bio-Rad) and visualized in the ChemiDoc MP System (1708280, Bio-Rad). Protein amounts were quantified with densitometry by using Image J. Optical densities were normalized with values determined on β-actin blots.

Statistical Analysis

For statistical data comparison, GraphPad Prism 9 was used. Differences between groups were analyzed by unpaired *t*-tests followed by Welch's corrections. All values are given as means ± standard deviations (SD), with *n* values indicating the number of samples or animals analyzed. Throughout the study, *p* values < 0.05 were considered significant.

Results

Adult Mice Are More Resistant to Ischemic Stroke Than Young Mice

LDF above the core of the MCA territory revealed no significant differences in regional CBF between young
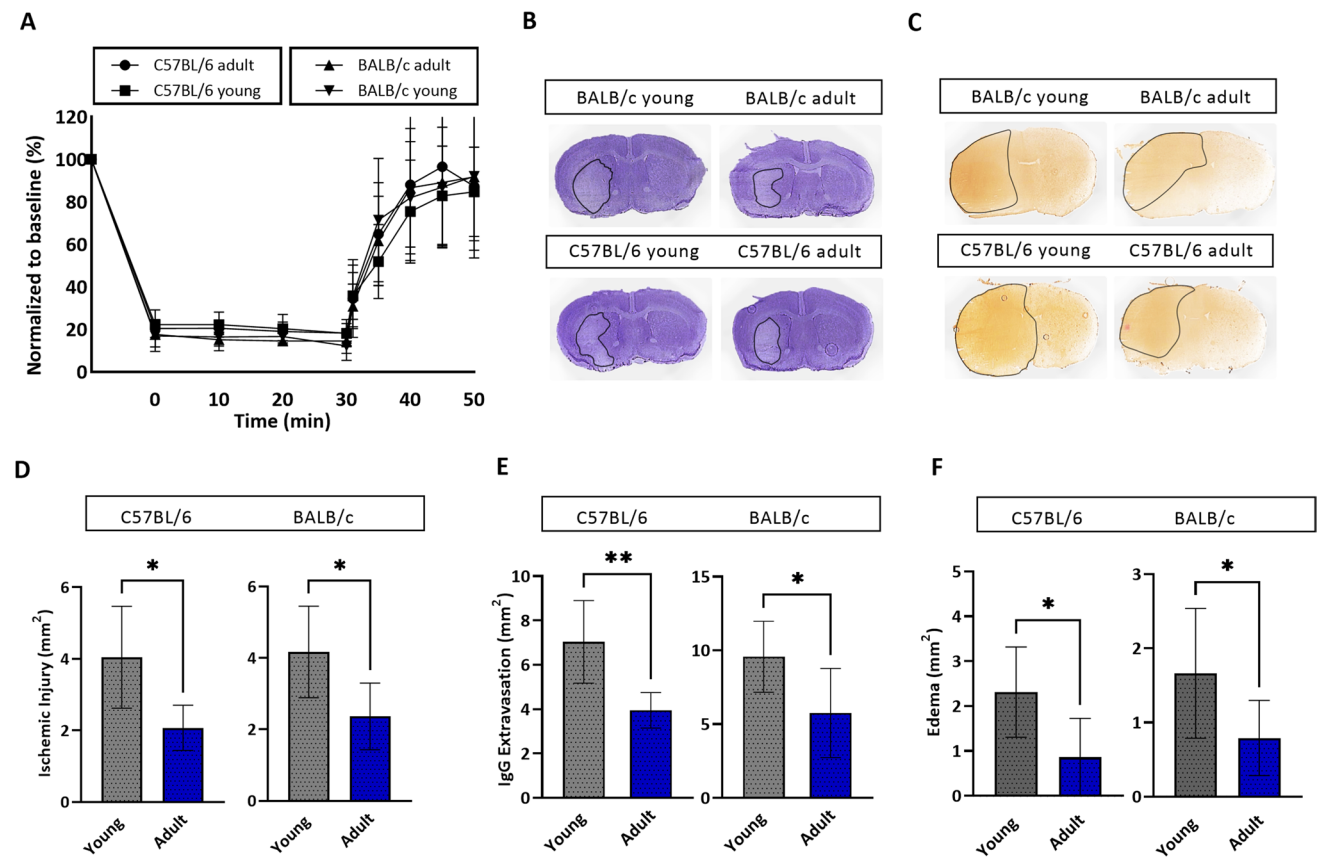

Fig. 1 Ischemic injury is attenuated in the brains of adult compared with young C57BL/6 and BALB/c mice. **A** Cerebral blood flow (CBF) measured via laser Doppler flowmetry (LDF) during ischemia and at the onset of reperfusion, **B** representative Cresyl violet stainings, **C** representative immunohistochemistries for extravasated serum IgG, **D** infarct area assessed in Cresyl violet stainings, **E** blood-brain barrier (BBB) leakage assessed by IgG immunostainings, and **F** brain edema area assessed by Cresyl violet stainings of young (9–12-week-old) and adult (72-week-old) C57BL/6 and BALB/c mice exposed to 30 min middle cerebral artery occlusion (MCAo), followed by 72 h reperfusion. Note that the severity of ischemias and post-ischemic reperfusion assessed by LDF (in **A**) did not differ between groups. Infarct areas are outlined in **B**. Note the difference in infarct size in young and adult mice. Data are mean ± SD values (*n*=7 mice/group). **p*<0.05/***p*<0.01 compared with corresponding young mice

and adult mice, both in the C57BL/6 and BALB/c strains. Regional CBF decreased to ~20% during MCAo and was rapidly restored to baseline after reperfusion (Fig. 1A). All young and adult BALB/C mice survived within 72 h after MCAo. There were two dead animal in the adult C57BL/6 group, one of them was in 1 h and the other one was in the 48th hour. Also, there was one dead animal in

the young C57BL/6 group in the 48th hour. Considering that we had established a well-defined model, in which the severity of ischemia did not differ between young and adult mice, we next assessed the ischemic injury and blood-brain barrier (BBB) integrity on Cresyl violet and anti-IgG-stained brain sections. Infarct area (Fig. 1B) and IgG extravasation (Fig. 1C), a marker of BBB leakage
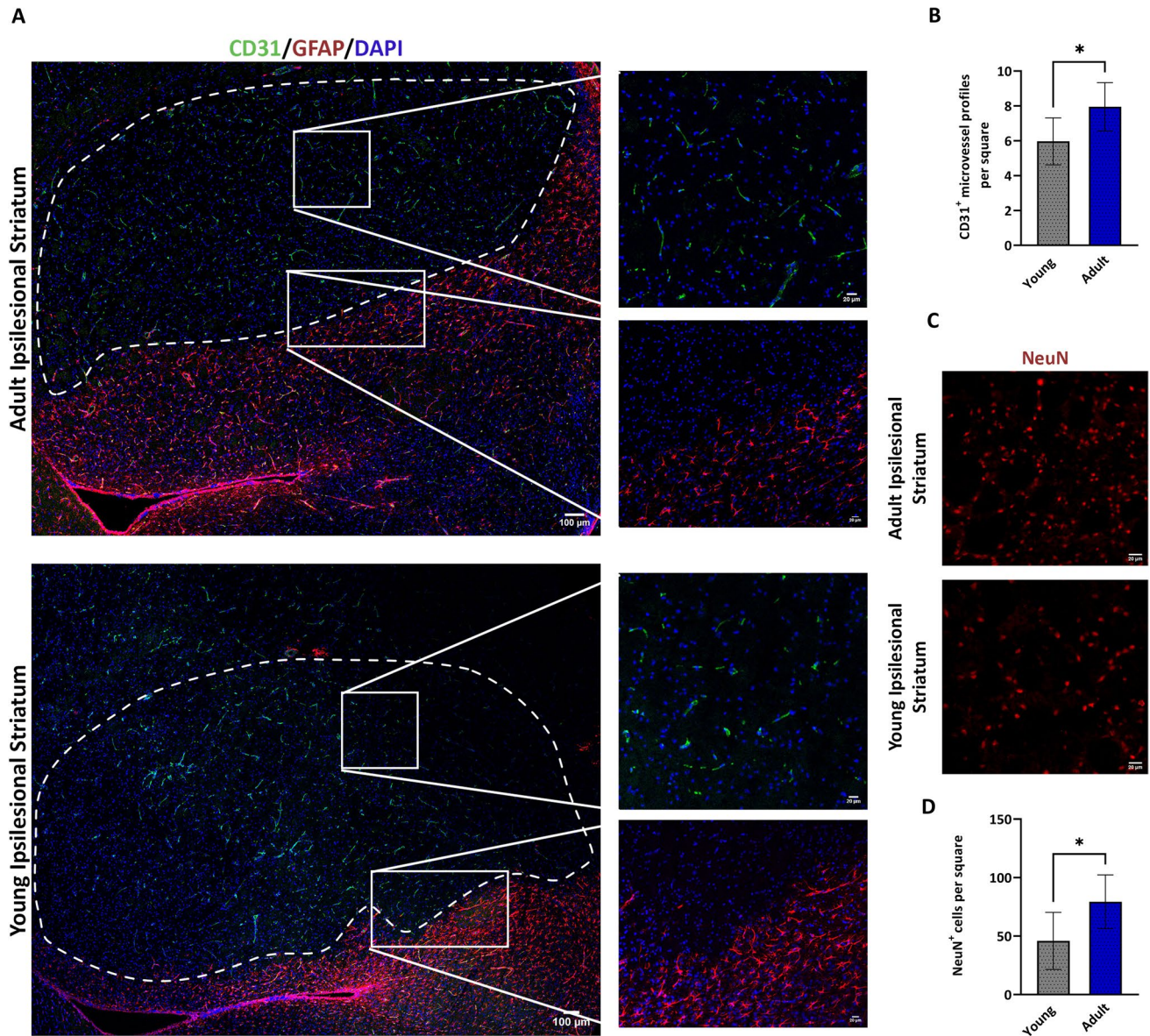
Fig. 2 Cerebral microvasculature is better protected against ischemia in adult compared with young mice, which is accompanied by better neuronal survival. **A**, **B** Brain microvascular density in the ischemic striatum was examined by CD31 immunohistochemistry and **C**, **D** NeuN$^+$ cells in the ischemic striatum were shown by NeuN immunohistochemistry of young (9–12-week-old) and adult (72-week-old) C57BL/6 mice exposed to 30 min MCAo, followed by 72 h reperfusion. Representative microphotographs are shown in **A** and **C**, and quantitative analyses in **B** and **D**. For infarct visualization, reactive GFAP$^+$ astrocytes (in red) and cell nuclei (in blue) were colabeled by GFAP immunohistochemistry and DAPI in **A** (CD31$^+$ microvessels in green). Infarct borders have been outlined by a dashed line. Data are mean ± SD values (n= mice/group). *$p<0.05$ compared with corresponding young mice. Scale bars: 100 μm (low magnification) and 20 μm (high magnification) images in **A** and 20 μm (high magnification) images in **C**
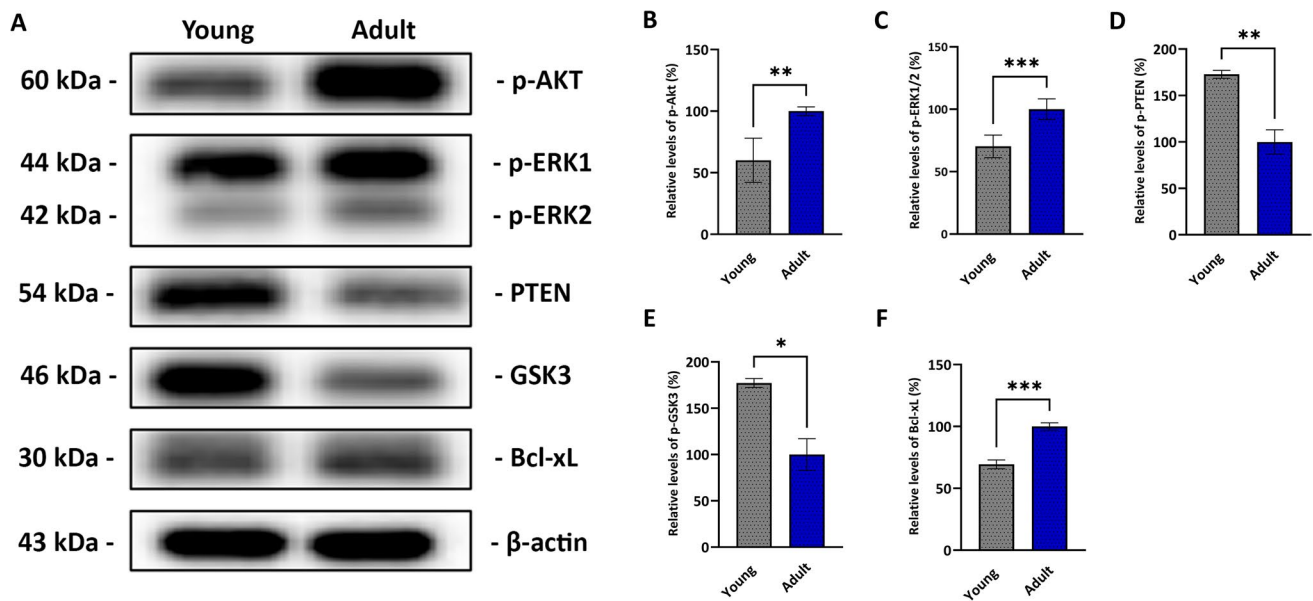
Fig. 3 Cell survival pathways are activated more strongly post-ischemia in adult than young mice. Western blot analysis of proteins involved in cell survival. **A** Representative Western blots for phosphorylated Akt (p-Akt), phosphorylated ERK-1/2 (p-ERK1/2), phosphorylated PTEN (p-PTEN), phosphorylated GSK3β (p-GSK3β), antiapoptotic Bcl-xL, and the housekeeping protein β-actin in the ischemic striatum of young (9–12-week-old) and adult (72-week-old) C57BL/6 mice exposed to 30 min MCAo, followed by 72 h reperfusion. Densitometric analysis revealed that (**B**) phosphorylated Akt (p-Akt) and (**C**) phosphorylated ERK-1/2 (p-ERK1/2), which mediate cell survival, were increased, while (**D**) phosphorylated PTEN (p-PTEN) and (**E**) phosphorylated GSK3β (p-GSK3β), which are associated with cell injury, were reduced, while (**F**) antiapoptotic Bcl-xL was increased in adult compared with young mice. All data were normalized to β-actin abundance. Data are mean ± SD values (*n*=3 independently processed blots per group). *$p<0.05$/**$p<0.01$/***$p<0.001$ compared with corresponding young mice

[33], were less pronounced in adult than young mice; this effect was not strain-dependent. Indeed, quantitative analysis revealed that adult mice exhibited significantly smaller infarct area (Fig. 1D), less IgG extravasation (Fig. 1E), and smaller edema area (Fig. 1F) in adult than young C57BL/6 and BALB/c mice. Since we evaluated that C57BL/6 and BALB/c gave the same response to ischemic stroke, we continued with C57BL/6 mice in the rest of the experiments.

Next, we analyzed the microvascular density in the non-ischemic contralesional striatum by CD31 immunohistochemistry and found that microvascular density was lower in adult than young mice (Suppl. Fig. 1A, B). However, upon ischemic stroke, the situation switched, and microvascular density was higher in the lesion-sided striatum of adult compared with young mice (Fig. 2A, B). We defined the infarct boundary by GFAP staining in peri-infarct zone and corpus callosum [34]. This observation indicates that the resilience of brain microvessels against ischemic injury was higher in adult than young mice.

We next investigated the effect of intraluminal MCAo on neuronal survival in the ischemic striatum by NeuN immunohistochemistry. The percentage of surviving NeuN+ neurons in the ischemic striatum was higher in adult than young mice (Fig. 2C, D), indicating that adult mice were better protected against ischemic stroke. We confirmed that there is no significant difference of NeuN+ cells in the contralesional striatum of adult and young mice (Suppl. Fig. 1C).

Cell Survival Pathways Are More Strongly Activated in the Ischemic Brain of Adult Compared with Young Mice

To further determine the underlying mechanisms of cell survival, we determined the responses of cell survival-associated proteins. The expression of phosphorylated Akt, phosphorylated ERK1/2, phosphorylated PTEN, phosphorylated GSK3β, and Bcl-xL proteins were measured by Western blotting. Protein levels of phosphorylated Akt and phosphorylated ERK1/2, which are associated with cell survival [35], were significantly higher in the ischemic striatum of adult than young mice (Fig. 3B, C); whole phosphorylated PTEN and phosphorylated GSK3β, which are associated with cell injury, were significantly lower in adult compared with
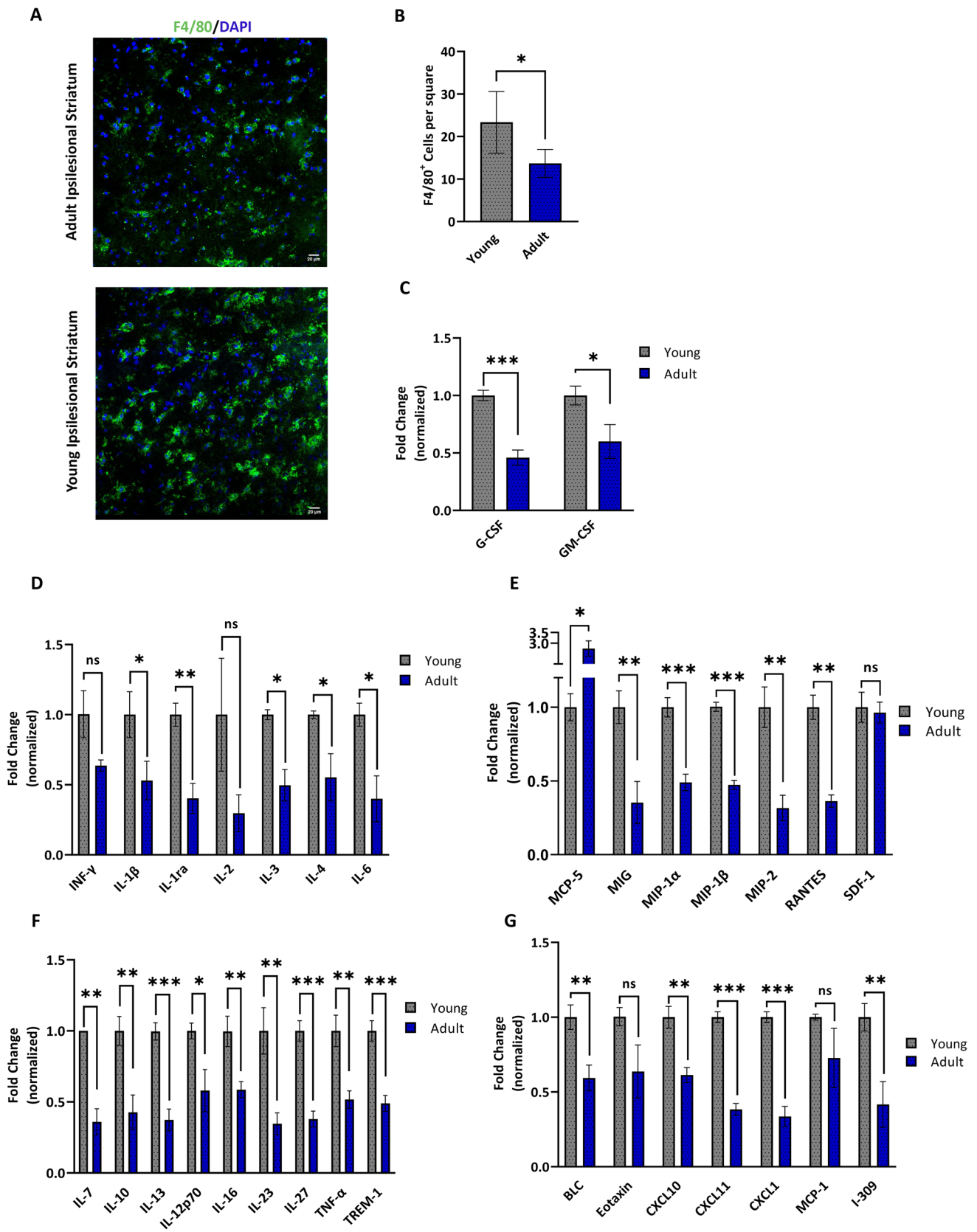
young mice (Fig. 3D, E). Moreover, anti-apoptotic Bcl-xL protein levels were significantly higher in the ischemic striatum of adult compared with young mice (Fig. 3F). Taken together, these studies exhibited a cell signaling response pattern favoring post-ischemic tissue survival.

Microglia/Macrophage Responses Are More Restricted in the Brain of Adult Than Young Mice, Resulting in Attenuated Cytokine and Chemokine Levels

Microglial cells are first-line defenders against ischemic brain injury, which sense danger-associated molecular patterns following stroke [36]. We thus compared the density of activated F4/80+ microglia/macrophages in the ischemic striatum of young and adult mice. We saw that the density of F4/80+-activated microglia/macrophages was significantly lower in the ischemic striatum of adult than young mice (Fig. 4A, B). Hence, we next determined the level of G-CSF and GM-CSF, which are growth factors that induce the proliferation and differentiation of microglia/macrophages [37]. We observed significantly decreased levels of G-CSF and GM-CSF in the ischemic striatum of adult compared with young mice (Fig. 4C). We next evaluated the levels of inflammatory cytokines and chemokines. We observed that the pro -and anti-inflammatory cytokines IL-1β, IL-1ra, IL-3, IL-4, IL-5, IL-6, IL-7, IL-10, IL-12p70, IL-13, IL-16, IL-17, IL-23, and IL-27 were significantly lower in the ischemic striatum of adult than young mice, as were TNF-α and TREM-1 (Fig. 4D, E). Also, the chemokines I-309, BLC, eotaxin, CXCL10, CXCL11, CXCL1, MIG, MIP-1α, MIP-1β, MIP-2, and RANTES were significantly lower in the ischemic striatum of adult than young mice (Fig. 4F, G). Levels of MCP-1 and SDF-1 did not differ between young and adult mice, while MCP-5 levels were significantly higher in adult than young mice (Fig. 4G). Overall, immune responses were attenuated in the brains of adult compared with young mice in response to focal cerebral ischemia.

Proteome Analysis Identifies Pathways Involved in Glycogen Degradation and Mitochondrial Dysfunction, Which Are Differentially Regulated Post-Ischemia in the Brains of Young and Aged Mice

As ischemic stroke dramatically damaged the striatum and changed its protein expression [38], we identified several proteins that were similarly altered by the stroke in both age groups. In LC-MS/MS, all identification data were reliable and accurate. When comparing proteome changes, 111 proteins were differentially abundant in the ischemic striatum of young and adult mice, when selected based on the −log (p-value) >1.3 (that is, p-value <0.05) cutoff. To understand the biological functions of altered proteins we performed Gene Ontology analysis using the Panther tools. Proteins were associated with the following classes: chaperone, cytoskeletal protein, enzyme modulator, hydrolase, membrane traffic protein, oxidoreductase, transferase, and transporter (Fig. 5A). Few proteins belonged to ligase, transcription factor, and transfer/carrier protein. Molecular function analysis showed that most proteins were involved in the following pathways: catalytic activity, binding, signal transducer activity, structural molecule activity, and transporter activity (Fig. 5B). Among 111 proteins, 80 proteins were elevated and 31 proteins reduced in adult mice according to fold change (Fig. 5C, D). We showed the visa verse results in young mice (Suppl. Fig. 2).

To further evaluate the proteome profile of the ischemic striatum, we next plotted log twofold changes against the t test-derived negative log 10 p-values for all proteins differentially expressed in young and adult mice (Fig. 6A). We now defined the cut-off based on a >1.3-fold change in addition to the −log (p-value) >1.3 selection criterion and continued subsequent analysis with 64 proteins, of which 45 proteins were elevated and 19 reduced in adult mice. Then, we investigated the protein-protein interaction and identified 2 independent networks, in which HSPA8 (heat shock protein family A member 8; also known as heat shock protein-70, Hsp70) and PARK7 (Parkinson disease protein-7; also known as protein deglycase DJ1) had the most interactions with other proteins (Fig. 6B). We confirmed that PARK7 protein expression was higher in the ischemic striatum od adult mice than young mice (Suppl. Fig. 3). Ingenuity Pathway Analysis (IPA) showed that among the most strongly regulated canonical pathways, the two top pathways upregulated in adult mice were associated with glycogen degradation, whereas the only pathway downregulated in adult mice was associated with mitochondrial dysfunction (Fig. 6C).

Although intraluminal MCAo most strongly affected the ischemic striatum, the contralesional striatum also exhibited proteome changes. Thus, we determined 27 proteins that were differentially abundant in the contralesional striatum of young and adult mice (Suppl. Fig. 4). Compared with young mice, 9 proteins were increased and 18 proteins were decreased in adult mice.
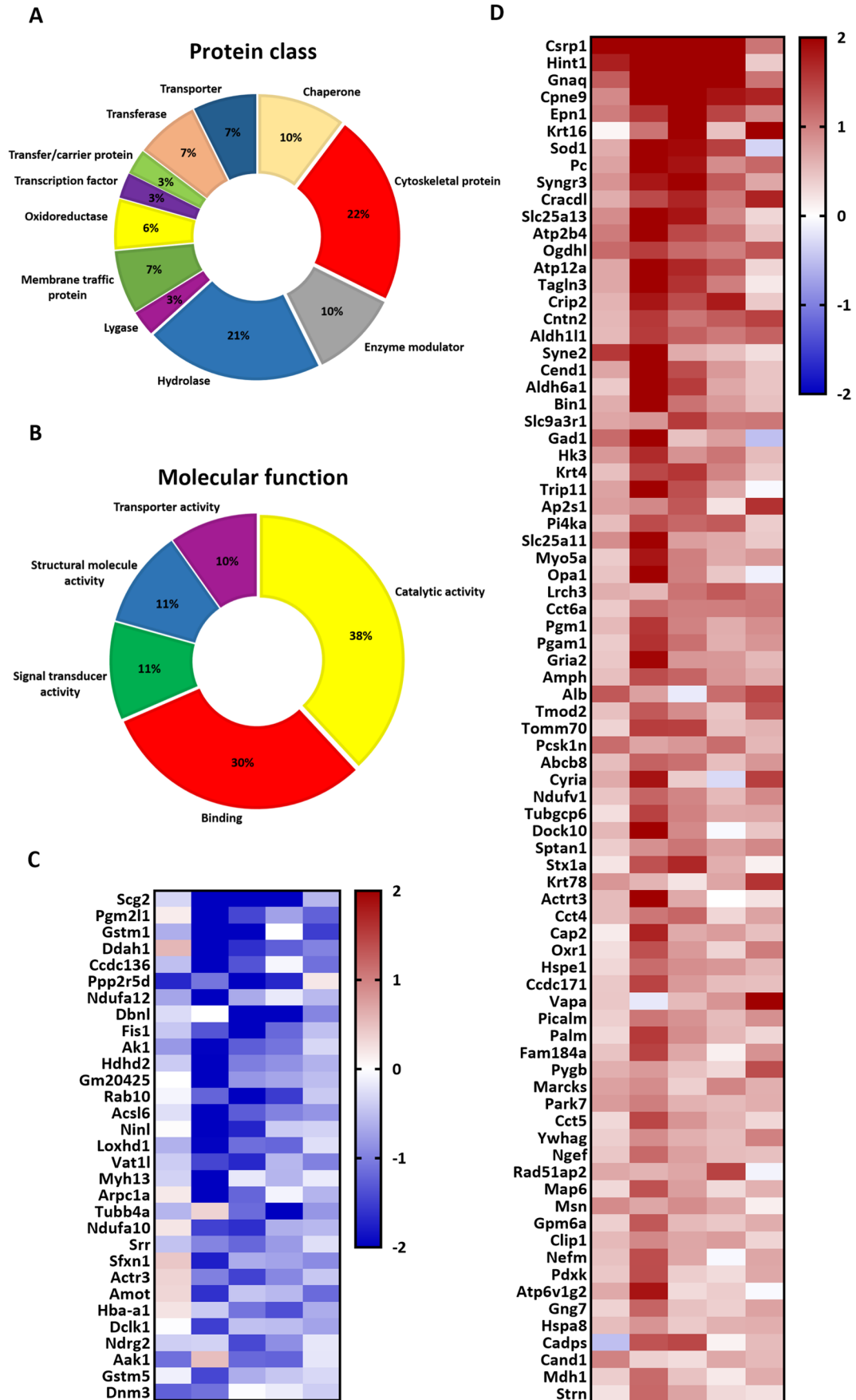
◄**Fig. 5** Aging profoundly alters proteome composition assessed by liquid chromatography-mass spectrometry (LC-MS/MS). Proteome analysis by LC-MS/MS in the ischemic striatum of young (9–12-week-old) and adult (72-week-old) C57BL/6 mice exposed to 30 min MCAo, followed by 72 h reperfusion. The most represented (**A**) protein classes and (**B**) molecular functions were categorized using Panther software. According to Gene Ontology enrichment analysis, results are shown as the percentage of proteins in pie charts. **C, D** Heatmaps of 111 differentially abundant proteins were selected based on a −log (*p*-value) >1.3 cutoff criterion, which was listed as log twofold changes. Eighty proteins were elevated and 31 proteins were reduced in adult compared with young mice. For protein representation, pseudocolors were used, dark red representing the highest protein abundance and dark blue the lowest protein abundance in adult compared with young mice

Discussion

By exposing young (9–12-week-old) and adult (72-week-old) BALB/c and C57BL/6 mice to 30 min of intraluminal MCAo, we herein show that although post-ischemic reperfusion, assessed by LDF, did not differ between young and adult mice, ischemic injury assessed by infarct area and IgG extravasation was smaller in adult than young mice. Microvascular survival and integrity assessed by CD31 immunohistochemistry and the neuronal survival shown by NeuN immunohistochemistry were higher in ischemic brain tissue of adult than young mice. Tissue protection was associated with stronger activation of cell survival pathways in adult than young mice. Microglial/macrophage activation assessed by F4/80 immunohistochemistry was reduced in adult compared with young mice. Interestingly, pro- and anti-inflammatory cytokine and chemokine responses were attenuated in adult mice. By means of LC-MS/MS, we identified a hitherto unknown proteome profile exhibiting the upregulation of glycogen degradation-related pathways and the downregulation of mitochondrial dysfunction-related pathways that distinguishes post-ischemic responses of the aged compared with the young brain. Our study suggests that aging increases the brain's resilience against ischemic injury.

A number of studies, including an own study, have previously shown that age increases the severity of ischemic injury in the mouse and rat brain [9, 12, 17, 18]. Two of these studies examined transient proximal (that is intraluminal) MCAo [9, 17] and two of these studies permanent distal MCAo [12, 18]. In our own study using the intraluminal MCAo model, we observed that post-ischemic reperfusion assessed by LDF was significantly reduced in adult compared with young mice [9]. Importantly, none of the other three studies reported LDF recordings or CBF measurements. The less complete reperfusion was likely responsible for the more severe injury in adult MCAo mice. In the present study, post-ischemic reperfusion assessed by LDF was not reduced in adult compared with young mice. The

lack of hemodynamic disturbances in adult mice enabled us to study post-ischemic injury development. We show that the severity of the ischemic injury was reduced in adult compared with young mice. This effect was strain-independent. Both C57BL/6 and BALB/c mice exhibited reduced infarct area, BBB leakage, and brain edema post-MCAo.

Microvascular density decreases during normal aging [39] confirmed this observation by demonstrating that the density of CD31+ brain microvessels was reduced in the non-ischemic striatum of adult compared with young mice. In response to MCAo, however, this situation switched and microvascular density was higher in the ischemic striatum of adult than young mice. These findings indicate that microvascular resistance to ischemia increased with aging. The increased microvascular viability and integrity were accompanied by increased neuronal survival, as shown by NeuN immunohistochemistry in the ischemic striatum, which represents the core of the MCA territory.

In Western blotting studies, we found that signaling pathways associated with cell survival were more strongly activated in the ischemic brain of adult than young mice. Under conditions of ischemic stroke, the phosphatidylinositol 3-kinase (PI3K)/Akt and ERK1/2 signal transduction pathways crucially control cell viability and homeostasis [35, 40]. In the ischemic striatum, the abundance of phosphorylated (that is, activated) Akt and phosphorylated (that is, activated) ERK1/2 was higher in adult than young mice, while the abundance of phosphorylated (that is, inactive) PTEN and phosphorylated (that is, inactive) GSK3β, which are inhibitory regulators of the PI3K/Akt signaling pathway [41], was reduced in adult mice. Bcl-xL is an antiapoptotic protein belonging to the Bcl-2 family that provides neuroprotection in ischemic stroke [42]. Bcl-xL abundance was significantly higher in the ischemic striatum of adult than young mice, in line with the enhanced survival of neurons in adult compared with young animals.

Immune responses critically influence ischemic injury in the reperfused ischemic brain [43]. Microglia are the first-line responders following ischemic injury, which release proinflammatory cytokines and chemokines that attract blood-derived leukocytes, including neutrophils, monocytes, and macrophages, to accumulate in the ischemic brain tissue [21]. By means of F4/80 immunohistochemistry, we observed a decreased number of activated microglia/macrophages in the ischemic brain of adult compared with young mice. Interestingly, levels of pro-and anti-inflammatory cytokines and chemokines were similarly reduced in the ischemic brain of adult compared with young mice, indicating an overall attenuation of immune responses associated with aging. Of note, alterations in the immune responses and immune cell compositions of aged compared with young brains have previously been shown after transient

intraluminal MCAo. Thus, in line with a reduced infarct area, reduced total leukocyte numbers were noted in the ischemic brain of old compared with young mice [13]. The leukocyte reduction particularly affected monocyte numbers, while brain-infiltrating neutrophils, which were increased in the peripheral blood of old compared with young mice, were relatively increased in the ischemic brain of old mice [13]. Monocytes and macrophages of old mice exhibited reduced phagocytic activity, as revealed by fluorescent bead uptake [13]. Although we did not evaluate brain leukocyte infiltrates in this study, our findings of attenuated microglia/macrophage accumulation and activation together with the reduced pro- and anti-inflammatory cytokine and chemokine

levels strengthen the idea that immune responses are attenuated post-ischemia in the adult brain.

Thirty minutes MCAo enable the investigate of cell signaling and protein chancing analysis since it is mild model of focal ischemia. We performed a large-scale proteomic analysis using LC-MS/MS to identify the changes in the protein profile of young and adult mice's ischemic and non-ischemic striatum. Thus, we identified 111 proteins that were differentially abundant in the young and adult brains. The proteins mostly belonged to chaperone, cytoskeletal protein, enzyme modulator, hydrolase, membrane traffic protein, oxidoreductase, transferase, and transporter classes. They were involved in catalytic activity, binding, signal transducer activity, structural
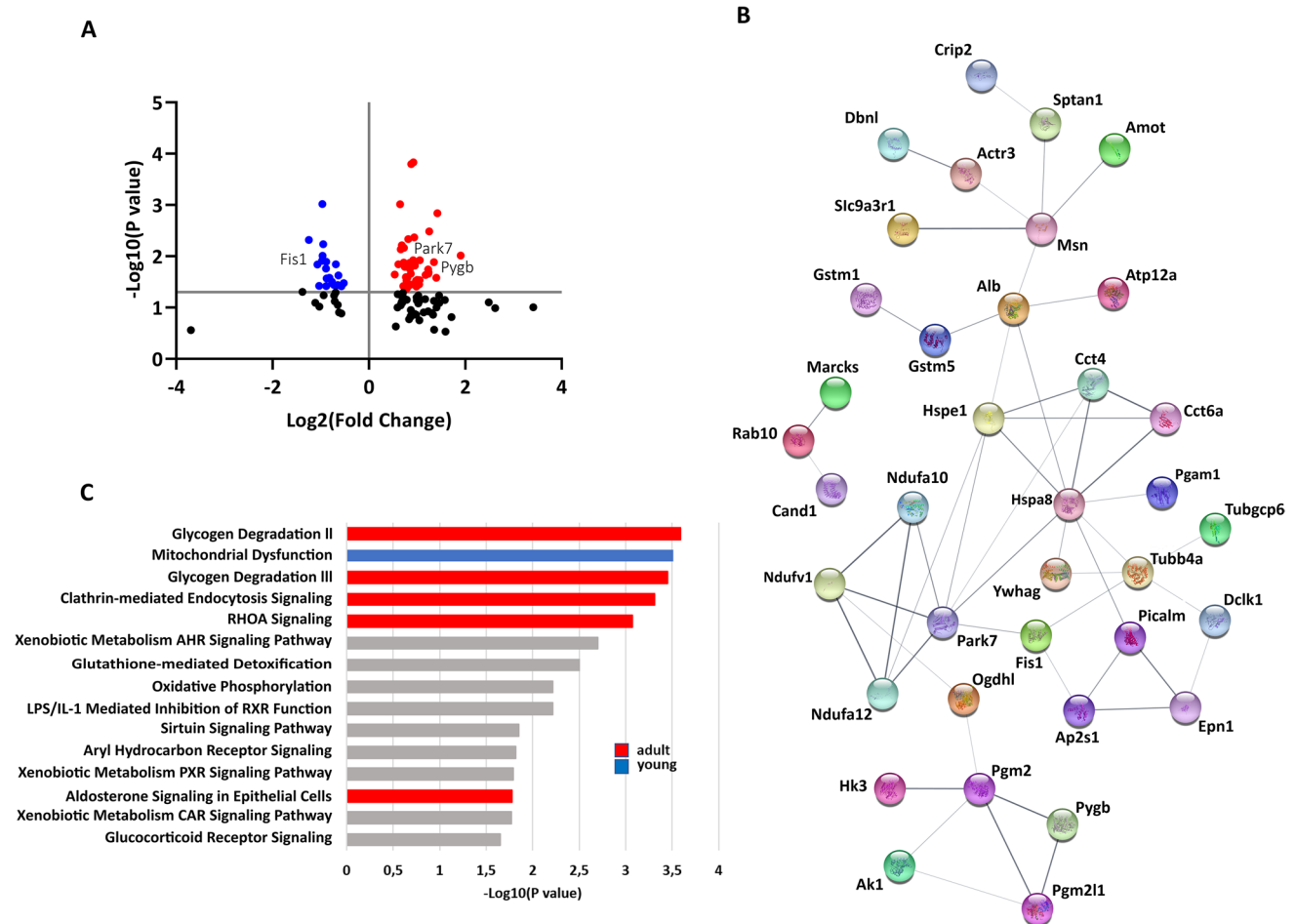

Fig. 6 Proteome profile distinguishes post-ischemic responses of the adult compared with the young brain. Computational pathway analysis of proteomic profiles of young and adult mice. **A** The log twofold change was plotted against the t test-derived negative log 10 p-value for all proteins differentially expressed in the striatum of young and adult mice. Elevated proteins in adult mice are indicated in red and reduced proteins are indicated in blue. **B** STRING protein-protein interaction network of 64 significantly elevated and reduced proteins selected based on a >1.3-fold change cutoff in addition to the −log (p-value) >1.3 criterion. Two independent modules were observed;

the confidence score was set at 0.4. **C** Ingenuity Pathway Analysis (IPA) denoting the top 15 canonical pathway categories and their t test-derived negative log 10 p-values. Categories upregulated in adult mice based on a −log (p-value) cutoff >3 are shown in red, and categories downregulated in adult mice based on the same cutoff are shown in blue. Note that the two top pathways upregulated in adult mice are associated with glycogen degradation and the only pathway downregulated in adult mice is associated with mitochondrial dysfunction

molecule activity, and transporter activity. Eighty proteins were increased in adult compared with young mice, and 31 proteins were reduced in adult mice. By means of protein-protein interaction analysis, we identified two independent networks, in which HSPA8 and PARK7 were found to have the most interactions with other proteins. HSPA8 (also known as Hsp70) is a heat shock protein acting as a chaperone in the ischemic brain [44] whereas PARK7 is a multifunctional protein with essential functions in mitochondrial homeostasis and cellular antioxidant responses [45]. It is noteworthy that both proteins were increased in the aged compared with the young ischemic brain, although HSPA8 was not significantly related to any canonical pathway in IPA. IPA showed that among the most strongly regulated canonical pathways, the two top pathways upregulated in adult mice were associated with glycogen degradation, whereas the only pathway downregulated in adult mice was associated with mitochondrial dysfunction. Glycogen storage and degradation have recently been recognized as key processes providing neuroprotection in ischemic stroke [46, 47]. Their role in age-related resilience against ischemic brain injury has so far been unknown. Further studies on age-related mechanisms of ischemic brain injury are warranted.

Conclusion

The pathophysiology of ischemic stroke is a highly complex process followed by secondary neuroinflammation involving oxidative stress and inflammatory reaction to promote further injury. We established the MCAo model using 72-week adult BALB/c and C57BL/6 mice to study the direct effect of aging. We revealed that adult mice were more resistant to ischemic stroke and developed better cell survival via signaling transduction. Besides, adult mice presented fewer cytokines and chemokines due to restricted microglia/macrophages in the ipsilesional striatum. Importantly, we showed alteration protein profiles between adult and young mice after ischemic stroke for the first time and concluded that age-related changes in energy metabolism might help diagnose and treat stroke.

Declarations

References

1. Katan M, Luft A (2018) Global burden of stroke. Semin Neurol 38(02):208–211. https://doi.org/10.1055/s-0038-1649503
2. Moretti A, Ferrari F, Villa RF (2015) Pharmacological therapy of acute ischaemic stroke: achievements and problems. Pharmacol Ther 153:79–89. https://doi.org/10.1016/j.pharmthera.2015.06.004
3. Benjamin EJ et al (2019) Heart disease and stroke statistics—2019 update: a report from the American Heart Association. Circulation 139(10). https://doi.org/10.1161/CIR.0000000000000659
4. Popa-Wagner A, Petcu EB, Capitanescu B, Hermann DM, Radu E, Gresita A (2020) Ageing as a risk factor for cerebral ischemia: underlying mechanisms and therapy in animal models and in the clinic. Mech Ageing Dev 190:111312. https://doi.org/10.1016/j.mad.2020.111312
5. Casals JB et al (2011) The use of animal models for stroke research: a review. Comp Med 61(4):305–313
6. Ma R et al (2020) Animal models of cerebral ischemia: a review. Biomed Pharmacother 131:110686. https://doi.org/10.1016/j.biopha.2020.110686
7. Palomeras Soler E, Casado Ruiz V (2010) Epidemiology and risk factors of cerebral ıschemia and ıschemic heart diseases: similarities and differences. Curr Cardiol Rev 6(3):138–149. https://doi.org/10.2174/157340310791658785
8. Jackson SJ et al (2017) Does age matter? The impact of rodent age on study outcomes. Lab Anim 51(2):160–169. https://doi.org/10.1177/0023677216653984
9. Wang C et al (2022) Postischemic neuroprotection associated with anti-ınflammatory effects by mesenchymal stromal cell-derived small extracellular vesicles in aged mice. Stroke 53(1). https://doi.org/10.1161/STROKEAHA.121.035821
10. Manwani B, Liu F, Xu Y, Persky R, Li J, McCullough LD (2011) Functional recovery in aging mice after experimental stroke. Brain Behav Immun 25(8):1689–1700. https://doi.org/10.1016/j.bbi.2011.06.015
11. Manwani B, Friedler B, Verma R, Venna VR, McCullough LD, Liu F (2014) Perfusion of ıschemic brain in young and aged animals. Stroke 45(2):571–578. https://doi.org/10.1161/STROKEAHA.113.002944
12. Fanxia S, Lidan J, Frank H, Vincent D, Shengdi C, Hua S (2018) Increased ınflammatory response in old mice is associated with more severe neuronal ınjury at the acute stage of ıschemic stroke. Aging Dis. https://doi.org/10.14336/AD.2018.0205
13. Ritzel RM et al (2018) Aging alters the immunological response to ischemic stroke. *Acta Neuropathol* 136(1):89–110. https://doi.org/10.1007/s00401-018-1859-2

14. Correa F et al (2011) Tissue plasminogen activator prevents white matter damage following stroke. J Exp Med 208(6):1229–1242. https://doi.org/10.1084/jem.20101880

15. Wang R-Y, Wang PS-G, Yang Y-R (2003) Effect of age in rats following middle cerebral artery occlusion. Gerontology 49(1):27–32. https://doi.org/10.1159/000066505

16. Won SJ et al (2006) Influence of age on the response to fibroblast growth factor-2 treatment in a rat model of stroke. Brain Res 1123(1):237–244. https://doi.org/10.1016/j.brainres.2006.09.055

17. DiNapoli VA, Huber JD, Houser K, Li X, Rosen CL (2008) Early disruptions of the blood–brain barrier may contribute to exacerbated neuronal damage and prolonged functional recovery following stroke in aged rats. Neurobiol Aging 29(5):753–764. https://doi.org/10.1016/j.neurobiolaging.2006.12.007

18. Popa-Wagner A, Badan I, Walker L, Groppa S, Patrana N, Kessler C (2007) Accelerated infarct development, cytogenesis and apoptosis following transient cerebral ischemia in aged rats. Acta Neuropathol 113(3):277–293. https://doi.org/10.1007/s00401-006-0164-7

19. Di Napoli M, Shah IM (2011) Neuroinflammation and cerebrovascular disease in old age: a translational medicine perspective. J Aging Res 2011:1–18. https://doi.org/10.4061/2011/857484

20. Qin C et al (2019) Dual functions of microglia in ıschemic stroke. Neurosci Bull 35(5):921–933. https://doi.org/10.1007/s12264-019-00388-3

21. Qiu Y et al (2021) Immune cells in the BBB disruption after acute ıschemic stroke: targets for ımmune therapy? Front Immunol 12. https://doi.org/10.3389/fimmu.2021.678744

22. Neumann J et al (2015) Very-late-antigen-4 (VLA-4)-mediated brain invasion by neutrophils leads to interactions with microglia, increased ischemic injury and impaired behavior in experimental stroke. Acta Neuropathol 129(2):259–277. https://doi.org/10.1007/s00401-014-1355-2

23. Li H, You W, Li X, Shen H, Chen G (2019) Proteomic-based approaches for the study of ıschemic stroke. Transl Stroke Res 10(6):601–606. https://doi.org/10.1007/s12975-019-00716-9

24. Gu R-F et al (2021) Proteomic characterization of the dynamics of ıschemic stroke in mice. J Proteome Res 20(7):3689–3700. https://doi.org/10.1021/acs.jproteome.1c00259

25. Caglayan AB et al (2019) Acute and post-acute neuromodulation ınduces stroke recovery by promoting survival signaling, neurogenesis, and pyramidal tract plasticity. Front Cell Neurosci 13. https://doi.org/10.3389/fncel.2019.00144

26. Beker MC et al (2015) Effects of normobaric oxygen and melatonin on reperfusion injury: role of cerebral microcirculation. Oncotarget 6(31):30604–30614. https://doi.org/10.18632/oncotarget.5773

27. Beker M et al (2020) Lentivirally administered glial cell line-derived neurotrophic factor promotes post-ischemic neurological recovery, brain remodeling and contralesional pyramidal tract plasticity by regulating axonal growth inhibitors and guidance proteins. Exp Neurol 331:113364. https://doi.org/10.1016/j.expneurol.2020.113364

28. Beker MC et al (2018) Time-of-day dependent neuronal ınjury after ıschemic stroke: ımplication of circadian clock transcriptional factor Bmal1 and survival kinase AKT. Mol Neurobiol 55(3):2565–2576. https://doi.org/10.1007/s12035-017-0524-4

29. Wiśniewski JR, Zougman A, Nagaraj N, Mann M (2009) Universal sample preparation method for proteome analysis. Nat Methods 6(5):359–362. https://doi.org/10.1038/nmeth.1322

30. Haçarız O, Baykal AT, Akgün M, Kavak P, Sağıroğlu MŞ, Sayers GP (2014) Generating a detailed protein profile of *Fasciola hepatica* during the chronic stage of infection in cattle. Proteomics 14(12):1519–1530. https://doi.org/10.1002/pmic.201400012

31. Serhatli M, Baysal K, Acilan C, Tuncer E, Bekpinar S, Baykal AT (2014) Proteomic study of the microdissected aortic media in human thoracic aortic aneurysms. J Proteome Res 13(11):5071–5080. https://doi.org/10.1021/pr5006586

32. Acioglu C et al (2016) Toll like receptor 9 antagonism modulates spinal cord neuronal function and survival: direct versus astrocyte-mediated mechanisms. Brain Behav Immun 56:310–324. https://doi.org/10.1016/j.bbi.2016.03.027

33. Natah SS, Srinivasan S, Pittman Q, Zonghang Z, Dunn JF (2009) Effects of acute hypoxia and hyperthermia on the permeability of the blood-brain barrier in adult rats. J Appl Physiol 107(4):1348–1356. https://doi.org/10.1152/japplphysiol.91484.2008

34. Shimada IS, Borders A, Aronshtam A, Spees JL (2011) Proliferating reactive astrocytes are regulated by notch-1 in the peri-ınfarct area after stroke. Stroke 42(11):3231–3237. https://doi.org/10.1161/STROKEAHA.111.623280

35. Dent P (2014) Crosstalk between ERK, AKT, and cell survival. Cancer Biol Ther 15(3):245–246. https://doi.org/10.4161/cbt.27541

36. Anttila JE, Whitaker KW, Wires ES, Harvey BK, Airavaara M (2017) Role of microglia in ischemic focal stroke and recovery: focus on Toll-like receptors. Prog Neuropsychopharmacol Biol Psychiatry 79:3–14. https://doi.org/10.1016/j.pnpbp.2016.07.003

37. Okubo M et al (2016) Macrophage-colony stimulating factor derived from ınjured primary afferent ınduces proliferation of spinal microglia and neuropathic pain in rats. *PloS One* 11(4):e0153375. https://doi.org/10.1371/journal.pone.0153375

38. Shah FA et al (2018) Identification of proteins differentially expressed in the striatum by melatonin in a middle cerebral artery occlusion rat model—a proteomic and in silico approach. Front Neurosci 12. https://doi.org/10.3389/fnins.2018.00888

39. Xu X et al (2017) Age-related ımpairment of vascular structure and functions. Aging Dis 8(5):590. https://doi.org/10.14336/AD.2017.0430

40. Yu JSL, Cui W (2016) Proliferation, survival and metabolism: the role of PI3K/AKT/mTOR signalling in pluripotency and cell fate determination. Development 143(17):3050–3060. https://doi.org/10.1242/dev.137075

41. Georgescu M-M (2010) PTEN tumor suppressor network in PI3K-Akt pathway control. Genes Cancer 1(12):1170–1177. https://doi.org/10.1177/1947601911407325

42. Zhao H, Yenari MA, Cheng D, Sapolsky RM, Steinberg GK (2003) Bcl-2 overexpression protects against neuron loss within the ischemic margin following experimental stroke and inhibits cytochrome c translocation and caspase-3 activity. J Neurochem 85(4):1026–1036. https://doi.org/10.1046/j.1471-4159.2003.01756.x

43. Pawluk H et al (2020) The role of selected pro-ınflammatory cytokines in pathogenesis of ıschemic stroke. Clin Interv Aging 15:469–484. https://doi.org/10.2147/CIA.S233909

44. Dukay B, Csoboz B, Tóth ME (2019) Heat-shock proteins in neuroinflammation. Front Pharmacol 10. https://doi.org/10.3389/fphar.2019.00920

45. Zhang F et al (2021) PARK7 enhances antioxidative-stress processes of BMSCs via the ERK1/2 pathway. J Cell Biochem 122(2):222–234. https://doi.org/10.1002/jcb.29845

46. Magistretti PJ, Allaman I (2018) Lactate in the brain: from metabolic end-product to signalling molecule. Nat Rev Neurosci 19(4):235–249. https://doi.org/10.1038/nrn.2018.19

47. Bastian C et al (2019) Role of brain glycogen during ıschemia, aging and cell-to-cell ınteractions:347–361. https://doi.org/10.1007/978-3-030-27480-1_12